

In Vitro Alterations Do Not Reflect a Requirement for Host Cell Cycle Progression during *Plasmodium* Liver Stage Infection

Kirsten K. Hanson,^a Sandra March,^{b,c} Shengyong Ng,^d Sangeeta N. Bhatia,^{b,c,e,f} Maria M. Mota^a

Instituto de Medicina Molecular, Faculdade de Medicina da Universidade de Lisboa, Lisbon, Portugal^a; Health Sciences and Technology/Institute for Medical Engineering and Science, Massachusetts Institute of Technology, Cambridge, Massachusetts, USA^b; Broad Institute, Cambridge, Massachusetts, USA^c; Department of Biological Engineering, Massachusetts Institute of Technology, Cambridge, Massachusetts, USA^d; Howard Hughes Medical Institute, Koch Institute, and Electrical Engineering and Computer Science, Massachusetts Institute of Technology, Cambridge, Massachusetts, USA^e; Department of Medicine, Brigham and Women's Hospital, Boston, Massachusetts, USA^f

Prior to invading nonreplicative erythrocytes, *Plasmodium* parasites undergo their first obligate step in the mammalian host inside hepatocytes, where each sporozoite replicates to generate thousands of merozoites. While normally quiescent, hepatocytes retain proliferative capacity and can readily reenter the cell cycle in response to diverse stimuli. Many intracellular pathogens, including protozoan parasites, manipulate the cell cycle progression of their host cells for their own benefit, but it is not known whether the hepatocyte cell cycle plays a role during *Plasmodium* liver stage infection. Here, we show that *Plasmodium* parasites can be observed in mitotic hepatoma cells throughout liver stage development, where they initially reduce the likelihood of mitosis and ultimately lead to significant acquisition of a binucleate phenotype. However, hepatoma cells pharmacologically arrested in S phase still support robust and complete *Plasmodium* liver stage development, which thus does not require cell cycle progression in the infected cell *in vitro*. Furthermore, murine hepatocytes remain quiescent throughout *in vivo* infection with either *Plasmodium berghei* or *Plasmodium yoelii*, as do *Plasmodium falciparum*-infected primary human hepatocytes, demonstrating that the rapid and prodigious growth of liver stage parasites is accomplished independent of host hepatocyte cell cycle progression during natural infection.

Intracellular pathogens have evolved highly sophisticated mechanisms to adapt the host cell niche to accommodate their specific developmental needs. As cell cycle progression is a fundamentally important biological process that leads to many functional alterations in cells, it is not surprising that numerous intracellular pathogens manipulate the cell cycle progression of their host cells. While important and well-studied examples arise from viral and bacterial infections (reviewed in references 1 and 2), protozoan parasites, such as *Toxoplasma gondii* (3–5), *Trypanosoma cruzi* (6), *Eimeria bovis* (7), *Encephalitozoon* spp. (8), and *Leishmania major* (9), have all been suggested to modulate host cell cycle progression. Perhaps the most striking example of dependence on host cell cycle progression in protozoan parasites comes from the apicomplexans *Theileria annulata* and *Theileria parva*, which ensure their own propagation by transforming the lymphocytes and monocytes they infect (reviewed in reference 10). During continuous rounds of cell cycle progression and mitosis, they align themselves to the host mitotic spindle for distribution into both daughter cells during cytokinesis (11).

During the symptomatic blood stage of infection, *Plasmodium* spp., the apicomplexan parasites that cause malaria, grow inside erythrocytes, which themselves completely lack replicative capacity. However, the asymptomatic *Plasmodium* liver stages (or exoerythrocytic forms [EEFs]) grow inside hepatocytes, which are quiescent parenchymal cells of the liver that can readily reenter the cell cycle and undergo mitosis in response to cellular or organismal stimuli (reviewed in reference 12). Evidence from both transcriptional and posttranscriptional studies of infected cells suggests that *Plasmodium* liver stage parasites may alter host cell cycle progression. Microarray data from *Plasmodium berghei*-infected Hepa1-6 cells at time points during the first 24 h of development revealed modulation of several cell cycle-associated transcripts

that are indicative of a trend toward cell cycle inhibition (13), with induction of three Gadd45 isoforms, which can mediate a G₂/M checkpoint (14), and repression of D- and B-type cyclins, as well as subunit 1 of the anaphase-promoting complex. Recent work probing the abundance and posttranslational modifications of select proteins in *Plasmodium yoelii*-infected HepG2-CD81 cells 24 h postinfection has suggested the opposite, that infected cells are in a proproliferative state, with data showing activated retinoblastoma protein (Rb) and less abundant p53 in infected cells (15).

The liver stage is a key phase of population growth within the *Plasmodium* life cycle, as a single sporozoite will replicate inside a parasitophorous vacuole and generate up to tens of thousands of progeny. This remarkable parasite expansion occurs inside a single hepatocyte, and it is an obvious hypothesis that the parasite might derive benefit from inducing cell cycle progression in its host hepatocyte. As a mammalian cell prepares to enter mitosis, it will not only have undergone replication of its DNA but will also have increased the biomass of most cellular organelles, thus increasing the cellular resources at the parasite's disposal. As it was

Received 3 July 2014 Accepted 14 November 2014

Accepted manuscript posted online 21 November 2014

Citation Hanson KK, March S, Ng S, Bhatia SN, Mota MM. 2015. *In vitro* alterations do not reflect a requirement for host cell cycle progression during *Plasmodium* liver stage infection. *Eukaryot Cell* 14:96–103. doi:10.1128/EC.00166-14.

Address correspondence to Maria M. Mota, mmota@fm.ul.pt.

Supplemental material for this article may be found at <http://dx.doi.org/10.1128/EC.00166-14>.

Copyright © 2015, American Society for Microbiology. All Rights Reserved. doi:10.1128/EC.00166-14

unknown whether liver stage *Plasmodium* parasites manipulate the cell cycle of the hepatocytes they infect or whether host cell cycle progression plays a role in *Plasmodium* infection, we have investigated the relationship between liver stage *Plasmodium* development and host hepatocyte cell cycle progression both *in vitro* and *in vivo*.

MATERIALS AND METHODS

Plasmodium liver stage assays. All *in vitro* experiments were conducted in HepG2 cells routinely maintained in Dulbecco's modified Eagle medium (DMEM) supplemented with 10% fetal bovine serum (FBS) and 1% penicillin-streptomycin (PenStrep). Green fluorescent protein (GFP)-expressing *P. berghei* sporozoites (16) were isolated from the salivary glands of infected mosquitos, and 20,000 were added per well of 24-well plates to HepG2 cells and cultured for the desired time in the presence of 1:300 amphotericin B (Fungizone). Infected cells were processed and analyzed by flow cytometry as described in reference 17 or by microscopy. For *in vivo* assays, 100,000 GFP-expressing *P. berghei* or 100,000 GFP-expressing *P. yoelii* (18) sporozoites were injected intravenously into C57BL/6 mice. Livers were harvested at the desired time point, rinsed in phosphate-buffered saline (PBS), and then fixed in 4% paraformaldehyde (PFA) for 1 h at room temperature and stored in PBS with 0.1% sodium azide at 4°C until processing.

All *in vivo* protocols were approved by the internal animal care committee of the Instituto de Medicina Molecular and were performed according to national and European regulations.

MPCC and Plasmodium falciparum infection. Micropatterned coculture (MPCC) preparation and *P. falciparum* infection were carried out as described previously (19, 20). Briefly, glass-bottom 96-well plates were coated homogeneously with rat tail type I collagen (50 µg/ml) and subjected to soft-lithographic techniques to pattern the collagen into microdomains of 500-µm islands that mediate selective hepatocyte adhesion. To create MPCCs, cryopreserved primary human hepatocytes (Life Technologies) were pelleted by centrifugation at 100 × g for 6 min at 4°C, assessed for viability using trypan blue exclusion (typically, 70 to 90% excluded the dye), and seeded on collagen-micropatterned plates. Each well contained approximately 10,000 hepatocytes organized in colonies of 500 µm in serum-free DMEM with 1% PenStrep. Two to 3 h later, the cells were washed with serum-free DMEM–1% PenStrep, and the medium was switched to human hepatocyte culture medium. One day after seeding, 75,000 freshly dissected *P. falciparum* sporozoites were added to each well. Three hours after sporozoite addition, the cells were washed twice, and 7,000 3T3-J2 murine embryonic fibroblasts were seeded per well.

Immunofluorescence labeling and microscopy. (i) Hepatoma cells and MPCCs. Infected cells were fixed in 4% PFA for 10 min at room temperature (RT), permeabilized with 0.1% Triton X-100, blocked in 2% bovine serum albumin (BSA), and incubated with primary antibodies for 2 h at RT. After washing, appropriate secondary antibodies were added, along with Hoechst 33342, and the cells incubated for 1 h at RT; following 5 PBS washes, coverslips were mounted in Fluoromount for imaging.

(ii) Liver slices. Fifty-micrometer-thick liver slices were cut from PFA-fixed livers on a vibratome. Slices were washed in PBS and then blocked and permeabilized with 0.3% Triton X-100, 2% BSA for 1 h at RT. Primary antibodies were incubated overnight at 4°C, and after extensive PBS washing, the slices were incubated with the appropriate secondary antibodies, along with phalloidin-Alexa Fluor 660 (1:50) and Hoechst dye for 2 h at RT. After PBS washes, slices were mounted in Fluoromount for imaging.

All images were acquired on Zeiss confocal microscopes. The primary antibodies used were Anti-Ki67 (ab15580; Abcam) at 1:300, anti-S10-phosphorylated histone H3 (06-570; Millipore) at 1:500, anti-β-tubulin (AA2; Sigma) at 1:1,000, anti-GFP–Alexa Fluor 488 (A-21311; Invitrogen) at 1:300, and anti-merozoite surface protein-1 (MSP-1) (25.1 [21]) at 1:200.

Induction of S-phase stasis. One day after plating, HepG2 cells were incubated with aphidicolin (2 µg/ml) in 500 µl of complete medium per well of a 24-well plate for 48 h. Immediately prior to infection, the cells were washed 3 times in PBS and switched to aphidicolin-free complete medium. EEF development was assessed by flow cytometry 48 h after sporozoite addition. For confirmation of S-phase stasis, cells were subjected to a 48-h aphidicolin treatment followed by washout, and a further 48 h later, cells were ethanol fixed and stained with propidium iodide in the presence of RNase A and then immediately analyzed by flow cytometry. Processing and analysis of all flow cytometry data were done with FlowJo.

EdU labeling. For HepG2 labeling, 10 µg/ml 5-ethynyl-2'-deoxyuridine (EdU; Life Technologies) was added to the medium at 24 h post-infection. MPCCs were incubated with 10 µg/ml EdU starting 3 h after sporozoite addition through to day 5.5 of infection, with fresh EdU-containing medium added daily. *In vivo*, C57BL/6 mice were infected intravenously (i.v.) with 200,000 GFP-expressing *P. berghei* or GFP-expressing *P. yoelii* sporozoites. One hundred fifty milligrams of EdU in PBS was injected intraperitoneally (i.p.) per mouse at the desired time points. Livers were harvested and fixed in 4% PFA at the time points indicated. Click-EdU fluorescent labeling in liver slices and cells was carried out according to the manufacturer's recommended protocol, followed by immunofluorescence labeling as described above.

Statistics. To assess whether infection altered the probability of a cell being mitotic, 2-by-2 contingency tables were analyzed in GraphPad Prism and two-tailed *P* values calculated at the 95% confidence interval using the chi-square test. Figure 1C was made using Forest Plot Viewer (http://ntp.niehs.nih.gov/go/tools_forestplotviewer). The percentage of infected versus noninfected binucleate cells at 48 h was analyzed with Student's *t* test.

RESULTS AND DISCUSSION

We first sought to establish whether *Plasmodium* parasites could be found in mitotic cells, using a standard *in vitro* model of infection in transformed, continuously cycling cells. To that end, we infected HepG2 human hepatoma cells with GFP-expressing *P. berghei* sporozoites. Coverslips with infected cells were fixed 24 and 48 h postinfection and immunostained for microscopy analysis using an antibody specific for the S10-phosphorylated form of histone H3, a marker of mitotic cells. EEFs could be observed in mitotic cells at both 24 and 48 h postinfection (Fig. 1A and B), demonstrating that mitosis and *Plasmodium* infection are not fundamentally incompatible processes *in vitro*. Since infected cells undergoing mitosis could be found during liver stage development, we next asked whether we could detect any evidence that cell cycle progression in the host HepG2 cell was being altered by infection. We compared infected and noninfected cell populations from the same coverslips, so that exposure to mosquito debris (inherent to the isolation of sporozoites from the salivary glands of infected mosquitos) was equivalent for both infected and noninfected cells. At 24 h postinfection, the likelihood that an infected cell would be mitotic was significantly less than the likelihood that a noninfected cell would be ($P < 0.0001$) (Fig. 1C). At 48 h postinfection, however, the likelihood of mitosis in infected and noninfected cells was not significantly different ($P = 0.3553$) (Fig. 1C). These data suggest that infection may initially reduce host cell cycle progression during the first 24 h after sporozoite invasion but that this reduction is transient and the rates of mitosis in infected and noninfected populations are equivalent by the end of the second day of infection.

There are several potential confounders for this analysis. HepG2 cells are plated at a density that both supports relatively efficient sporozoite invasion and keeps the cells largely subconfluent even at 48 h postinfection, as is seen in the image in Fig. 1A.

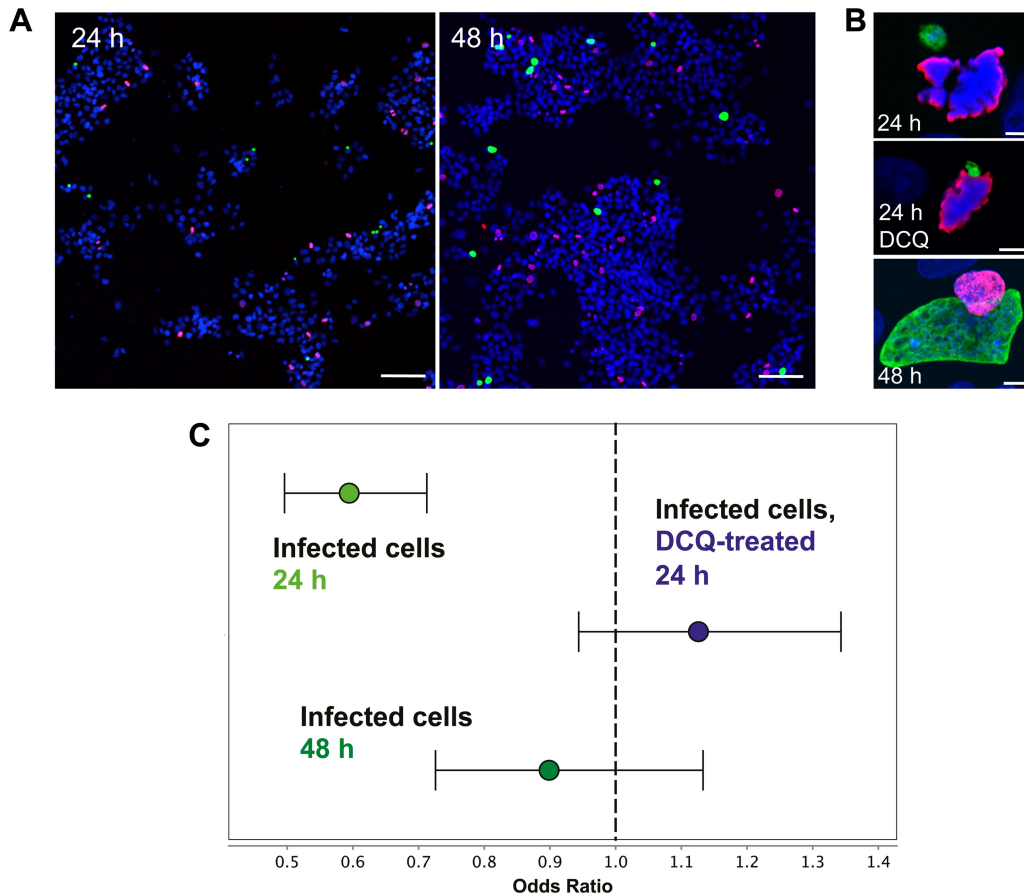


FIG 1 *P. berghei*-infected HepG2 cells undergo mitosis with some alteration of the mitotic index. (A) Representative low-magnification view of HepG2 landscape (nuclei shown by Hoechst labeling, in blue) of mitosis (phosphorylated histone H3-Ser 10, in red) and infection (EEFs, in green) at 24 h and 48 h postinfection. Scale bar = 100 μ m. (B) Representative images of infected, mitotic cells (24 h postinfection, 24 h postinfection with a decoquinate treatment [DCQ] from 2 to 8 h, and 48 h postinfection) with nuclei shown in blue, phosphorylated histone H3-Ser 10 in red, and the parasite in green. Scale bar = 5 μ m. (C) Odds ratios of the likelihood of mitosis in infected cells determined 24 h and 48 h postinfection and in decoquinate-treated cells 24 h postinfection. Error bars represent the 95% confidence interval (CI). At 24 h after sporozoite addition, 754 mitotic cells were identified from 23,145 total noninfected cells analyzed, while 142 mitotic cells were identified from 7,236 total infected cells (odds ratio, 0.5944, and 95% CI, 0.4959 to 0.7126; $P < 0.0001$, chi-square test). At 48 h postinfection, 633 mitotic cells were identified from 22,932 total noninfected cells, while 100 mitotic cells were found in 4,020 infected cells analyzed (odds ratio, 0.8987, and 95% CI, 0.7258 to 1.1330; $P = 0.3533$, chi-square test). In decoquinate-treated cells 24 h after sporozoite addition, 639 mitotic cells were identified from 20,882 total noninfected cells analyzed, while 160 mitotic cells were identified from 4,663 total infected cells (odds ratio, 1.12, and 95% CI, 0.9437 to 1.3430; $P = 0.1880$, chi-square test).

Still, local or global cell density may affect the likelihood that a given cell will undergo mitosis or be invaded by a sporozoite. Additionally, HepG2 cells in different stages of the cell cycle may have an altered likelihood of invasion. Recent work has demonstrated that sporozoites show no preference for actively cycling hepatocytes *in vivo* but do seem to preferentially invade cells of higher ploidy both *in vitro* and *in vivo* (22). For the *in vitro* situation, this would translate to a greater proportion of cells in G₂, which have already replicated DNA in preparation for mitosis, in the infected versus noninfected populations; such a bias for invading G₂ cells might also explain the strong reduction in the likelihood that a host cell 24 h postinfection will be mitotic. To address both of these issues, we asked whether the likelihood of mitosis in the host cell would be similarly altered at 24 h in cells harboring nondeveloping parasites that had undergone normal invasion. To block parasite development as early as possible after invasion, we treated cells with decoquinate (DCQ), a cytochrome *bc*₁ inhibitor and potent antimalarial (23, 24) that is active against very early liver stages, such that a 6-h treatment from 2 to 8 h after sporozoite

addition prevents parasite growth but does not lead to parasite elimination (25). A representative image of such a DCQ-treated parasite in a metaphase HepG2 cell 24 h postinfection is shown in Fig. 1B. If the reduction in the proportion of mitotic infected cells we observed was dependent on either spatial relationships between cell density and invasion or sporozoite preference for invading cells in a particular stage of the cell cycle, we would expect to see a similarly reduced likelihood of mitosis in the DCQ-treated infected cells at 24 h. Quite strikingly, this was not the case; the association between infection and a reduced likelihood of mitosis is lost in the DCQ-treated infected cells at 24 h postinfection ($P = 0.188$) (Fig. 1C). DCQ-treated infected cells are in fact somewhat more likely than noninfected cells to be mitotic, though this difference does not achieve statistical significance. These data strongly indicate that factors which may bias sporozoite invasion do not underlie the reduced likelihood of mitosis in infected cells at 24 h and that, instead, an actively growing parasite is required.

While our data clearly demonstrate that HepG2 cells harboring liver stage *Plasmodium* parasites do undergo mitosis, albeit with

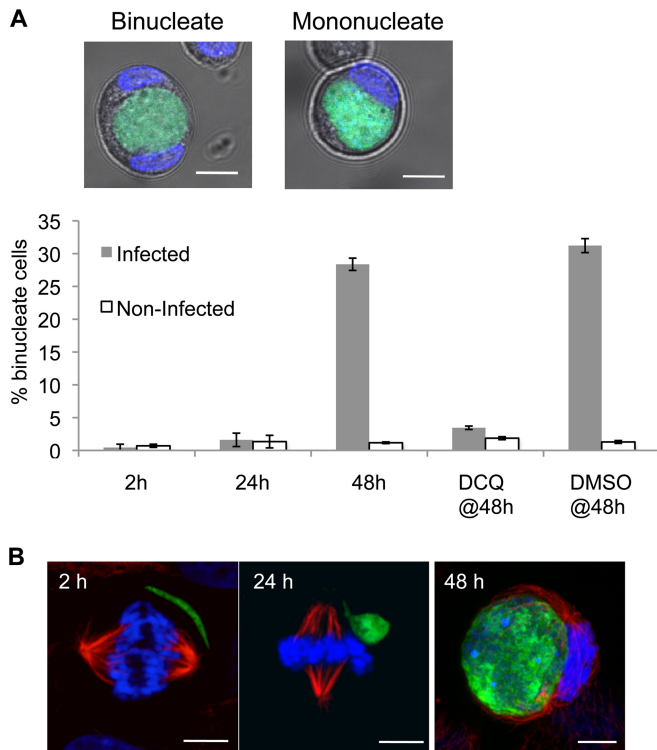


FIG 2 Growing *P. berghei* schizonts induce host cell binuclearity and associate with the mitotic spindle *in vitro*. (A) Mono- or binuclearity of infected cells was determined by live imaging of freshly trypsinized HepG2 cells 2 h and 24 h postinfection and 48 h postinfection with and without a 6-h decoquinate treatment during early parasite development. Images show representative confocal slices through binucleate and mononucleate infected cells 48 h postinfection, with GFP-expressing *P. berghei* in green and nuclei (Hoechst) in blue, along with bright-field images of the cells. Bars represent the mean percentages of binuclearity of infected and noninfected cells at 2, 24, or 48 h postinfection, with drug treatment as indicated. DCQ or DMSO (vehicle control) treatment was from 2 to 8 h postinfection, followed by washout. Error bars represent the standard deviations of the results from 3 independent experiments. (B) Representative confocal images (projections of z stacks spanning the EEF and the spindle) of 2 h, 24 h, and 48 h EEFs developing in mitotic HepG2 cells. Infected HepG2 cells were PFA fixed and labeled with anti-GFP antibody (EEF, green), anti- β -tubulin antibody (red), and Hoechst (nuclei, blue). Scale bar = 5 μ m in all panels.

decreased likelihood at 24 h postinfection, they do not provide information about whether mitosis in these infected cells is successful. While analyzing the mitotic state of infected cells at 48 h postinfection, we noted, as have others (26), the presence of clearly binucleate infected cells, suggestive of cytokinesis failure. To quantify this phenotype throughout liver stage infection, we trypsinized HepG2 cells infected with GFP-expressing *P. berghei* 2, 24, and 48 h after sporozoite addition and determined the percentage of binuclearity in infected versus noninfected cells by live microscopy after Hoechst labeling. Trypsinization causes cells to detach from the monolayer and round up, allowing clear discrimination of both cell boundaries and the number of nuclei present in each cell. At 2 and 24 h postinfection, both infected and noninfected cells were overwhelmingly mononucleate (Fig. 2A). Strikingly, though, at 48 h postinfection, an average of 28% of infected cells had acquired a binucleate phenotype, in contrast with the 1% binuclearity seen in noninfected cells from the same population, a highly significant difference ($P = 1.61E^{-5}$) (Fig. 2A). This binu-

cleate phenotype is almost completely lost if parasite development is arrested by brief DCQ treatment from 2 to 8 h postinfection; only 3% of DCQ-treated infected cells were binucleate at 48 h, compared with 2% in the noninfected population (Fig. 2A). As expected, nearly a third of infected cells at 48 h (31%) that had received a 6-h vehicle control treatment with dimethyl sulfoxide (DMSO) were binucleate (Fig. 2A). Given that infected cells were almost exclusively mononucleate at 24 h, the substantial proportion of binucleate cells harboring large schizonts at 48 h further indicates that many infected HepG2 cells do actively progress through the cell cycle during the second day of liver stage infection, though they do not necessarily complete cytokinesis successfully. β -Tubulin staining of infected cells supports the idea that only large schizonts cause cytokinesis failure; EEFs do not associate with the mitotic spindle of the infected cell at 2 or 24 h postinfection, nor do they appear to be positioned so that they would obstruct the formation of the cleavage furrow. At 48 h postinfection, though, spindles can be observed stretched around EEFs in tight apposition (Fig. 2B), leaving the parasite positioned such that successful cytokinesis to generate two daughter cells would require cleavage of the parasite as well. This association with the mitotic spindle is probably due to the space constraints inside a HepG2 cell harboring a replicating schizont, rather than a direct attempt by the parasite to manipulate the spindle at this stage. While the likelihood of mitosis in a 48-h infected cell is not different from that of a noninfected cell, the parasite appears to provide a substantial obstruction to cytokinesis as it becomes progressively larger during schizogony from 24 to 48 h postinfection. Infected cells most likely undergo mitosis with successful karyokinesis but fail in cytokinesis, leading to a significant proportion of binucleate infected cells at 48 h, which presumably also have increased ploidy.

Hepatocytes *in vivo* are capable of both increases and reductions in chromosome copies and number of nuclei during mitosis (27), with incomplete cytokinesis the mechanism underlying increases in ploidy (28). An increase in cellular ploidy could be beneficial to the parasite; indeed, a recent report has provided evidence that *Plasmodium* sporozoites preferentially invade cells with a ploidy greater than 2N, though the basis for this preference remains unknown (22). The *in vitro* alterations we observe in host cell cycle progression during infection raise the possibility that *Plasmodium* liver stages harness the host cell cycle to generate an advantageous environment for their own replication and growth.

To directly test whether EEF development requires host cell cycle progression and the presumed increase in ploidy accompanied by the acquisition of binuclearity observed in many infected cells, we sought to pharmacologically block host cell cycle progression after sporozoite invasion had occurred. Unsurprisingly, compounds capable of blocking HepG2 cell cycle progression by interfering with either the cytoskeleton or DNA replication, such as aphidicolin, also directly block the replication of the rapidly developing EEF (29, 30). Some cell types, however, are known to respond to the prolonged DNA replication fork stalls induced by extended aphidicolin treatment by arresting permanently in S phase after drug washout, a phenotype termed S-phase stasis (31). Fortuitously, HepG2 cells enter S-phase stasis after a 48-h treatment with 2 μ g/ml aphidicolin, with a majority of cells remaining viable and still blocked in S phase after an additional 48 h of incubation in drug-free complete medium (Fig. 3A); thus, we infected aphidicolin-blocked cells to test whether host cell cycle progression is required for *Plasmodium* growth. Strikingly, parasite

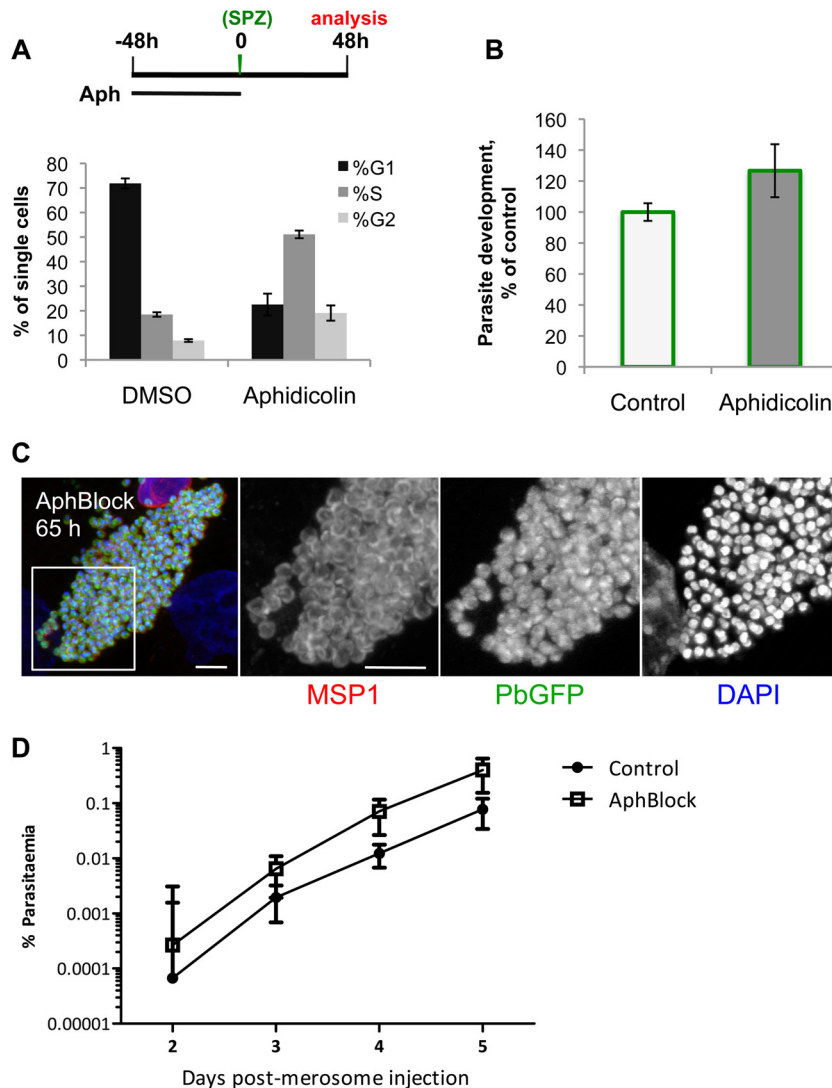


FIG 3 Host cell cycle progression is not required for robust and complete liver stage *Plasmodium* development *in vitro*. (A) Schematic illustrates experimental setup for aphidicolin block. At 48 h after aphidicolin washout, HepG2 cells were propidium iodide labeled and profiled by flow cytometry to determine the percentage of single cells in the G₁, S, and G₂-M phases of the cell cycle. Data (means \pm standard deviations) shown are from one representative experiment with technical quadruplicate wells with at least 10,000 cells processed per well. (B) Aphidicolin block was performed as described for panel A; 48 h after aphidicolin washout and GFP-expressing *P. berghei* sporozoite infection, the geometric mean amounts of GFP (a quantitative readout of parasite growth) from the control and aphidicolin-treated cells were determined by flow cytometry. Data represent the means and standard deviations of the results of 3 independent experiments. (C) Aphidicolin block (AphBlock) was performed as described for panel A, but infection was allowed to proceed for 65 h before cells were fixed and immunolabeled with MSP-1, shown in red in the left-most panel, anti-GFP antibody (PbGFP, GFP-expressing *P. berghei*), in green, and DAPI (nuclei), in blue. The white square inset in the merged image of mature hepatic merozoites delineates the area presented at higher magnification in separate grayscale images for each of the three labels. The images are projections of confocal slices through the parasite (scale bars = 5 μ m). (D) Two hundred microliters (of 500 μ l total) of merosome-containing medium from aphidicolin-blocked or control HepG2 cells 65 h postinfection with GFP-expressing *P. berghei* sporozoites was injected i.v. into C57BL/6 mice, and blood stage infection was subsequently monitored by flow cytometry from day 2 through day 5 after merosome injection. Each point represents the mean parasitemia of 5 animals; error bars represent standard deviations.

growth is completely unimpaired in aphidicolin-blocked HepG2 cells (Fig. 3B). As some cells do appear to escape S-phase stasis and progress in the cell cycle (as can be seen from the data in Fig. 3A), we wanted to ensure that it was not only these “escaper” cells that were able to support EEF growth. We used metabolic EdU labeling, initiated 24 h after sporozoite infection, to confirm that robust EEF development occurs specifically in those cells which remain in S-phase stasis and do not incorporate any EdU. In the DMSO-treated control, most cells are actively synthesizing DNA (EdU positive) during the window from 24 to 48 h postinfection,

and these cells support robust parasite growth (see Fig. S1 in the supplemental material). Conversely, the majority of aphidicolin-blocked cells are EdU negative but are also still capable of supporting robust parasite growth (see Fig. S1). EEFs undergo extensive DNA synthesis during the EdU treatment window but do not noticeably incorporate EdU. This is presumably because the liver stage parasite is unable to salvage pyrimidines, as has been demonstrated for the asexual blood stages (32); the modified nucleotide is likely unable to cross the parasitophorous vacuole membrane and/or the parasite plasma membrane.

The final step of *Plasmodium* liver stage development is the release of merosomes filled with mature merozoites into the sinusoidal circulation (18, 33). Aphidicolin-blocked cells support the production of mature merozoites, with merozoite surface protein-1 (MSP-1) properly localized to the periphery of each individual merozoite at 65 h postinfection (Fig. 3C). In HepG2 cells, the merosome release step results in detachment of merozoite-containing host cells from the monolayer, with the merozoites from these detached cells capable of initiating blood stage infection (33). Sixty-five hours after infection with GFP-expressing *P. berghei* sporozoites, the culture medium, which should contain merosomes/detached cells, was collected from 5 individual wells of both aphidicolin-blocked and control cells and injected intravenously into C57BL/6 mice. Analyzing 1 million erythrocytes by flow cytometry, blood stage parasitemia was first detectable 2 days after merosome injection in animals receiving either control or aphidicolin-blocked merosomes and rose steadily each day (Fig. 3D). Altogether, these data demonstrate that although *P. berghei* infection initially reduces the likelihood that a cell will be mitotic and leads to the acquisition of a binucleate phenotype, host cell cycle progression *per se* is not required for complete liver stage development *in vitro* in HepG2 cells.

Ultimately, though, natural *Plasmodium* infection at this stage in the life cycle occurs in the mammalian liver, where hepatocytes are not transformed and continually cycling but quiescent (in G_0) and capable of reentering the cell cycle in response to a variety of stimuli. In order to definitively test the hypothesis that cell cycle progression is not required for *Plasmodium* liver stage infection, we turned first to a rodent infection model. As less than 1% of hepatocytes in the rodent liver are cycling under normal conditions (34) and sporozoites do not preferentially invade those cycling hepatocytes (22), if *Plasmodium* infection would cause hepatocytes to reenter the cell cycle, this would be possible to detect by analyzing relatively small numbers of infected hepatocytes for signs of mitosis or cell cycle progression during parasite schizogony. No infected hepatocytes ($n > 1,000$) were observed to be mitotic 44 to 48 h after infection with *P. berghei* sporozoites, based on the morphology of DAPI- or Hoechst-labeled host cell nuclei in liver slices from either C57BL/6 or BALB/c mice. However, in the best-studied example of hepatocyte reentry into the cell cycle, the 2/3 partial hepatectomy model, the peak of DNA synthesis (S phase) in mice occurs 36 h after the triggering event, surgical liver resection (35). Using this timing of cell cycle progression as a guide, if sporozoite invasion or host cell remodeling during the early liver stages were to induce hepatocytes to reenter the cell cycle, infected cells would likely be in G_2 or perhaps still in S phase during late EEF schizogony, one possible explanation for the absence of mitotic figures in infected cells. To address whether *Plasmodium* infection would induce cell cycle progression in infected hepatocytes in the murine liver, we performed metabolic EdU labeling in the mouse to check whether infected hepatocytes were replicating their DNA at several time points during parasite schizogony. *P. berghei*-infected cells were uniformly EdU negative at both 24 h and 48 h after infection (Fig. 4A and Table 1); as expected, EdU-positive noninfected hepatocytes were rare (0.3% EdU positive in 2,477 analyzed).

We additionally confirmed that hepatocytes infected with *P. yoelii*, a species which undergoes more rapid development than *P. berghei* and generates more merozoites (36), were also not engaged in DNA synthesis up to 46 h after infection (Fig. 4A and

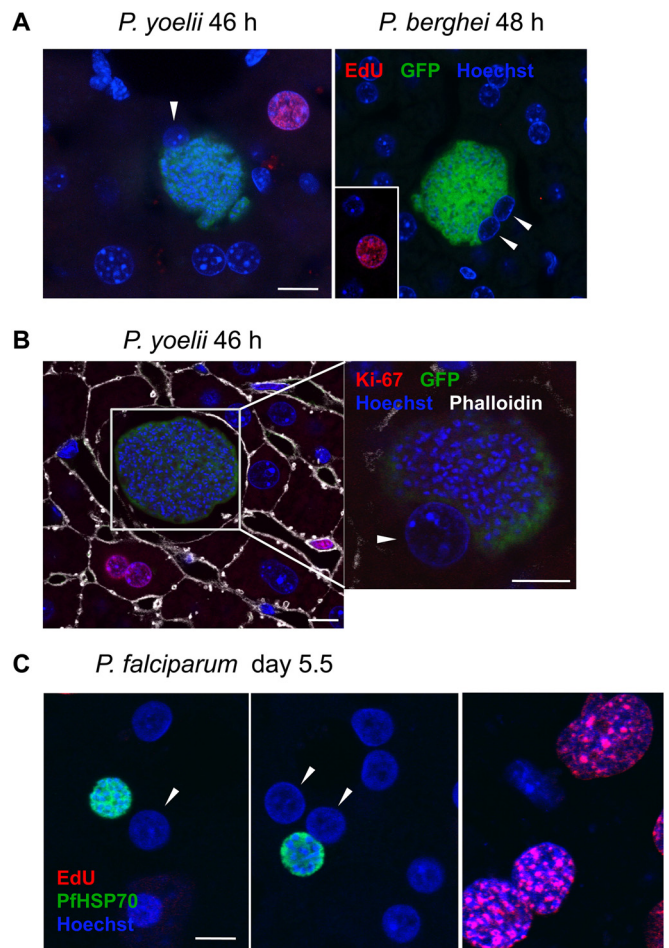


FIG 4 Infected hepatocytes do not reenter the cell cycle in response to *P. berghei* or *P. yoelii* infection *in vivo* or *P. falciparum* infection *ex vivo*. (A) EdU injected i.p. during either *P. berghei* or *P. yoelii* liver stage infection readily labels cells synthesizing DNA, including rare hepatocytes (next to an infected cell in the left panel showing *P. yoelii* and from a noncontiguous region of liver, as indicated, in the right panel showing *P. berghei*), but host hepatocyte nuclei, indicated by white arrowheads, were EdU negative. Representative confocal images are shown; quantification of the results is presented in Table 1. Bar = 10 μm . Pseudocoloring is as indicated by colors of labels. (B) Cells in the liver, including hepatocytes, are labeled by the G_1 -M marker Ki67, but infected hepatocytes (white arrowhead) are uniformly Ki67 negative. Representative *P. yoelii* EEF at 46 h postinfection are shown; the white box in the left panel indicates the area shown in a different z section, containing a nucleus of the infected cell, magnified in the right panel. Images are single confocal slices. Pseudocolouring is as indicated by colors of labels. Scale bars = 10 μm . (C) Human hepatocytes do not incorporate EdU during *P. falciparum* infection, though supportive stromal cells in MPCCs do. Representative confocal images show infected binucleate (left) and mononucleate (middle) hepatocytes and stromal cells (right). The nuclei of infected hepatocytes are indicated by white arrowheads. Pseudocolouring is as indicated by colors of labels. Anti-PfHSP70, *P. falciparum* heat shock protein 70 was used to mark EEFs. Bar = 10 μm for all panels.

Table 1). While infected murine hepatocytes did not enter S phase during *Plasmodium* development, it remained possible that the infected hepatocytes could reenter the cell cycle and progress to a G_1 state, prior to the onset of DNA synthesis. Ki67 immunolabeling of infected liver slices, to mark all cells in the G_1 -M phases of the cell cycle, was used to specifically address whether infected cells were in G_1 , as our data had already ruled out the possibility

TABLE 1 Quantification of EdU labeling in infected murine hepatocytes *in vivo* and human hepatocytes *ex vivo*

Parasite species	Time of EdU exposure (h p.i. ^a or as indicated)	Time analyzed (h p.i. or as indicated)	Infected hepatocytes with EdU ⁺ nuclei/total analyzed
<i>P. berghei</i>	23	24	0/27
<i>P. berghei</i>	24	48	0/58
<i>P. berghei</i>	40	48	0/38
<i>P. yoelii</i>	24	46	0/35
<i>P. yoelii</i>	40	46	0/44
<i>P. falciparum</i>	Throughout infection in culture medium	Day 5.5 p.i.	0/35

^a p.i., postinfection.

that cells were in S, G₂, or M phase. Again, while rare cycling hepatocytes could be observed (0.47% Ki67 positive in 1,292 analyzed), none of those containing *P. berghei* (0/15) or *P. yoelii* (0/29) EEFs were stained by Ki67, corroborating the EdU results and ruling out progression into G₁ (Fig. 4B). These data definitively demonstrate that infected murine hepatocytes do not reenter the cell cycle in response to *Plasmodium* EEF development *in vivo* and, thus, that the host cell cycle progression is not required during liver stage *Plasmodium* infection in the mouse model.

While both *P. berghei* and *P. yoelii* efficiently infect and complete liver stage development in C57BL/6 mice, with injection of 1,000 sporozoites of either species being sufficient to ensure blood stage parasitemia in naive animals (37), *Mus musculus* is of course not the natural host for either *P. berghei* or *P. yoelii*. These parasites infect African thicket rats (*Grammomys surdaster* and *Thamnomys rutilans*), and we cannot exclude the possibility that hepatocytes from the natural host could respond differently to *Plasmodium* infection than those of the laboratory mouse. To extend our analysis to a natural host-parasite combination and to the *Plasmodium* parasite responsible for most human malaria mortality, we turned to an *ex vivo* model of *P. falciparum* liver stage development. This model uses micropatterned cocultures of primary human hepatocytes and supporting stromal cells (MPCCs) to better recapitulate *in vivo* hepatocyte physiology (19). Hepatocytes in this format maintain a functional phenotype for up to 4 to 6 weeks without replication, as assessed by major liver-specific functions and gene expression, and they support complete *P. falciparum* liver stage development (19, 20). Using this MPCC system, we infected primary human hepatocytes grown in glass-bottom 96-well plates with freshly isolated *P. falciparum* sporozoites. MPCCs were then cultured in the presence of 10 μg/ml EdU, starting 3 h after sporozoite addition and continuing through day 5.5 of infection, with medium and EdU replenished daily. As seen by the images in Fig. 4C, infected primary human hepatocytes, both binucleate and mononucleate, failed to incorporate EdU; all infected cells we observed were EdU negative (Table 1). Importantly, and as expected, the uninfected primary hepatocytes were uniformly EdU negative, while many of the surrounding stromal cells did incorporate EdU (Fig. 4C). Though *P. falciparum* EEFs in MPCCs do not grow to the same large size as *in vivo*, these EEFs do form infectious merozoites (20), allowing us to conclude that host hepatocyte cell cycle progression is also not required for complete *P. falciparum* liver stage development.

In summary, our data demonstrate that, although *Plasmodium* liver stage infection initially leads to reduced likelihood of mitosis and ultimately to frequent acquisition of binuclearity as a result of

cytokinesis failure in transformed hepatoma cells *in vitro*, cell cycle progression is not required for complete *P. berghei* liver stage development. Most crucially, neither *P. falciparum*, *P. berghei*, nor *P. yoelii* parasites induce quiescent, nontransformed hepatocytes to reenter the cell cycle in response to infection.

Liver stage infection does clearly cause profound changes in cell cycle progression in infected HepG2 cells *in vitro*, which undoubtedly both result from and give rise to alterations at the transcript and protein levels in the infected cells. However, the cellular changes we have identified *in vitro* appear to be completely non-adaptive from the parasite's point of view. While changes in individual gene expression, protein abundance, or posttranslational modifications inside an infected hepatocyte that are associated with different stages of the cell cycle may yet prove critical for the parasite to complete development, cell cycle progression itself is not required for liver stage infection *in vitro* or *in vivo*. While *in vitro* infection models using transformed cell lines have led to many important breakthroughs in host-pathogen interactions, our results accentuate the importance of interrogating the functional significance of features of host cell biology such as cell cycle progression in experimental setups that mimic the natural state of the infected cell as closely as possible.

ACKNOWLEDGMENTS

We thank Ana Parreira in the Mota laboratory for mosquito production and infection and Anthony A. Holder (NIMR) for kindly providing anti-MSP-1 antibody. 3T3-J2 fibroblasts were courtesy of Howard Green (Harvard Medical School).

This work was supported by funding from the European Research Council under the European Union's 7th Framework Programme (FP7/2007-2013) through ERC grant agreement number 311502 (M.M.M.) and from Fundação para a Ciência e Tecnologia (FCT; Portugal) through grant number EXCL/IMI-MIC/0056/2012 (M.M.M.). K.K.H. was supported by funds from the European Community's Seventh Framework Programme (FP7/2007-2013) Marie Curie IEF (PIEF-GA-2008-221854) and Fundação para a Ciência e Tecnologia (SFRH/BPD/40989/2007).

REFERENCES

- Nascimento R, Costa H, Parkhouse RM. 2012. Virus manipulation of cell cycle. *Protoclasma* 249:519–528. <http://dx.doi.org/10.1007/s00709-011-0327-9>.
- Oswald E, Nougayrede JP, Taieb F, Sugai M. 2005. Bacterial toxins that modulate host cell-cycle progression. *Curr Opin Microbiol* 8:83–91. <http://dx.doi.org/10.1016/j.mib.2004.12.011>.
- Molestina RE, El-Guendy N, Sinai AP. 2008. Infection with *Toxoplasma gondii* results in dysregulation of the host cell cycle. *Cell Microbiol* 10:1153–1165. <http://dx.doi.org/10.1111/j.1462-5822.2008.01117.x>.
- Brunet J, Pfaff AW, Abidi A, Unoki M, Nakamura Y, Guinard M, Klein JP, Candolfi E, Mousli M. 2008. *Toxoplasma gondii* exploits UHRF1 and induces host cell cycle arrest at G2 to enable its proliferation. *Cell Microbiol* 10:908–920. <http://dx.doi.org/10.1111/j.1462-5822.2007.01093.x>.
- Lavine MD, Arrizabalaga G. 2009. Induction of mitotic S-phase of host and neighboring cells by *Toxoplasma gondii* enhances parasite invasion. *Mol Biochem Parasitol* 164:95–99. <http://dx.doi.org/10.1016/j.molbiopara.2008.11.014>.
- Costales JA, Daily JP, Burleigh BA. 2009. Cytokine-dependent and independent gene expression changes and cell cycle block revealed in *Trypanosoma cruzi*-infected host cells by comparative mRNA profiling. *BMC Genomics* 10:252. <http://dx.doi.org/10.1186/1471-2164-10-252>.
- Taubert A, Wimmers K, Ponsuksili S, Jimenez CA, Zahner H, Hermosilla C. 2010. Microarray-based transcriptional profiling of *Eimeria bovis*-infected bovine endothelial host cells. *Vet Res* 41:70. <http://dx.doi.org/10.1051/vetres/2010041>.
- Scanlon M, Shaw AP, Zhou CJ, Visvesvara GS, Leitch GJ. 2000. Infection by microsporidia disrupts the host cell cycle. *J Eukaryot Microbiol* 47:525–531. <http://dx.doi.org/10.1111/j.1550-7408.2000.tb00085.x>.

9. Kuzmenok OI, Chiang SC, Lin YC, Lee ST. 2005. Retardation of cell cycle progression of macrophages from G1 to S phase by ICAM-L from *Leishmania*. *Int J Parasitol* 35:1547–1555. <http://dx.doi.org/10.1016/j.ijpara.2005.08.006>.
10. Dobbelaere DA, Rottenberg S. 2003. Theileria-induced leukocyte transformation. *Curr Opin Microbiol* 6:377–382. [http://dx.doi.org/10.1016/S1369-5274\(03\)00085-7](http://dx.doi.org/10.1016/S1369-5274(03)00085-7).
11. von Schubert C, Xue G, Schmuckli-Maurer J, Woods KL, Nigg EA, Dobbelaere DA. 2010. The transforming parasite *Theileria* co-opts host cell mitotic and central spindles to persist in continuously dividing cells. *PLoS Biol* 8:e1000499. <http://dx.doi.org/10.1371/journal.pbio.1000499>.
12. Fausto N, Campbell JS, Riehle KJ. 2006. Liver regeneration. *Hepatology* 43:S45–S53. <http://dx.doi.org/10.1002/hep.20969>.
13. Albuquerque SS, Carret C, Grosso AR, Tarun AS, Peng X, Kappe SH, Prudencio M, Mota MM. 2009. Host cell transcriptional profiling during malaria liver stage infection reveals a coordinated and sequential set of biological events. *BMC Genomics* 10:270. <http://dx.doi.org/10.1186/1471-2164-10-270>.
14. Wang XW, Zhan Q, Coursen JD, Khan MA, Kontny HU, Yu L, Hollander MC, O'Connor PM, Fornace AJ, Jr, Harris CC. 1999. GADD45 induction of a G2/M cell cycle checkpoint. *Proc Natl Acad Sci U S A* 96:3706–3711. <http://dx.doi.org/10.1073/pnas.96.7.3706>.
15. Kaushansky A, Ye AS, Austin LS, Mikolajczak SA, Vaughan AM, Camargo N, Metzger PG, Douglass AN, MacBeath G, Kappe SH. 2013. Suppression of host p53 is critical for *Plasmodium* liver-stage infection. *Cell Rep* 3:630–637. <http://dx.doi.org/10.1016/j.celrep.2013.02.010>.
16. Franke-Fayard B, Trueman H, Ramesar J, Mendoza J, van der Keur M, van der Linden R, Sinden RE, Waters AP, Janse CJ. 2004. A *Plasmodium berghei* reference line that constitutively expresses GFP at a high level throughout the complete life cycle. *Mol Biochem Parasitol* 137:23–33. <http://dx.doi.org/10.1016/j.molbiopara.2004.04.007>.
17. Prudencio M, Rodrigues CD, Ataíde R, Mota MM. 2008. Dissecting in vitro host cell infection by *Plasmodium* sporozoites using flow cytometry. *Cell Microbiol* 10:218–224. <http://dx.doi.org/10.1111/j.1462-5822.2007.01032.x>.
18. Tarun AS, Baer K, Dumpit RF, Gray S, Lejarcegui N, Frevert U, Kappe SH. 2006. Quantitative isolation and in vivo imaging of malaria parasite liver stages. *Int J Parasitol* 36:1283–1293. <http://dx.doi.org/10.1016/j.ijpara.2006.06.009>.
19. Khetani SR, Bhatia SN. 2008. Microscale culture of human liver cells for drug development. *Nat Biotechnol* 26:120–126. <http://dx.doi.org/10.1038/nbt1361>.
20. March S, Ng S, Velmurugan S, Galstian A, Shan J, Logan DJ, Carpenter AE, Thomas D, Sim BK, Mota MM, Hoffman SL, Bhatia SN. 2013. A microscale human liver platform that supports the hepatic stages of *Plasmodium falciparum* and *vivax*. *Cell Host Microbe* 14:104–115. <http://dx.doi.org/10.1016/j.chom.2013.06.005>.
21. Holder AA, Freeman RR. 1982. Biosynthesis and processing of a *Plasmodium falciparum* schizont antigen recognized by immune serum and a monoclonal antibody. *J Exp Med* 156:1528–1538. <http://dx.doi.org/10.1084/jem.156.5.1528>.
22. Austin LS, Kaushansky A, Kappe SH. 2014. Susceptibility to *Plasmodium* liver stage infection is altered by hepatocyte polyploidy. *Cell Microbiol* 16:784–795. <http://dx.doi.org/10.1111/cmi.12282>.
23. da Cruz FP, Martin C, Buchholz K, Lafuente-Monasterio MJ, Rodrigues T, Sonnichsen B, Moreira R, Gamo FJ, Marti M, Mota MM, Hannus M, Prudencio M. 2012. Drug screen targeted at *Plasmodium* liver stages identifies a potent multistage antimalarial drug. *J Infect Dis* 205:1278–1286. <http://dx.doi.org/10.1093/infdis/jis184>.
24. Nam TG, McNamara CW, Bopp S, Dharia NV, Meister S, Bonamy GM, Plouffe DM, Kato N, McCormack S, Bursulaya B, Ke H, Vaidya AB, Schultz PG, Winzeler EA. 2011. A chemical genomic analysis of decoquinate, a *Plasmodium falciparum* cytochrome b inhibitor. *ACS Chem Biol* 6:1214–1222. <http://dx.doi.org/10.1021/cb200105d>.
25. Hanson KK, Ressurreicao AS, Buchholz K, Prudencio M, Herman-Ornelas JD, Rebelo M, Beatty WL, Wirth DF, Hanscheid T, Moreira R, Marti M, Mota MM. 2013. Torins are potent antimalarials that block replenishment of *Plasmodium* liver stage parasitophorous vacuole membrane proteins. *Proc Natl Acad Sci U S A* 110:E2838–E2847. <http://dx.doi.org/10.1073/pnas.1306097110>.
26. Stanway RR, Mueller N, Zobiak B, Graewe S, Froehle U, Zessin PJ, Aepfelbacher M, Heussler VT. 2011. Organelle segregation into *Plasmodium* liver stage merozoites. *Cell Microbiol* 13:1768–1782. <http://dx.doi.org/10.1111/j.1462-5822.2011.01657.x>.
27. Duncan AW, Taylor MH, Hickey RD, Hanlon Newell AE, Lenzi ML, Olson SB, Finegold MJ, Grompe M. 2010. The ploidy conveyor of mature hepatocytes as a source of genetic variation. *Nature* 467:707–710. <http://dx.doi.org/10.1038/nature09414>.
28. Guidotti JE, Bregerie O, Robert A, Debey P, Brechot C, Desdouets C. 2003. Liver cell polyploidization: a pivotal role for binuclear hepatocytes. *J Biol Chem* 278:19095–19101. <http://dx.doi.org/10.1074/jbc.M300982200>.
29. Fennell B, Naughton J, Barlow J, Brennan G, Fairweather I, Hoey E, McFerran N, Trudgett A, Bell A. 2008. Microtubules as antiparasitic drug targets. *Expert Opin Drug Discov* 3:501–518. <http://dx.doi.org/10.1517/17460441.3.5.501>.
30. Inselburg J, Banyal HS. 1984. Synthesis of DNA during the asexual cycle of *Plasmodium falciparum* in culture. *Mol Biochem Parasitol* 10:79–87. [http://dx.doi.org/10.1016/0166-6851\(84\)90020-3](http://dx.doi.org/10.1016/0166-6851(84)90020-3).
31. Borel F, Lacroix FB, Margolis RL. 2002. Prolonged arrest of mammalian cells at the G1/S boundary results in permanent S phase stasis. *J Cell Sci* 115:2829–2838.
32. Sherman IW. 1979. Biochemistry of *Plasmodium* (malaria parasites). *Microbiol Rev* 43:453–495.
33. Sturm A, Amino R, van de Sand C, Regen T, Retzlaff S, Renneberg A, Krueger A, Pollok JM, Menard R, Heussler VT. 2006. Manipulation of host hepatocytes by the malaria parasite for delivery into liver sinusoids. *Science* 313:1287–1290. <http://dx.doi.org/10.1126/science.1129720>.
34. Fabrikant JI. 1968. The kinetics of cellular proliferation in regenerating liver. *J Cell Biol* 36:551–565. <http://dx.doi.org/10.1083/jcb.36.3.551>.
35. Mitchell C, Willenbring H. 2008. A reproducible and well-tolerated method for 2/3 partial hepatectomy in mice. *Nat Protoc* 3:1167–1170. <http://dx.doi.org/10.1038/nprot.2008.80>.
36. Landau I, Killick-Kendrick R. 1966. Rodent plasmodia of the République Centrafricaine: the sporogony and tissue stages of *Plasmodium chabaudi* and *P. berghei yoelii*. *Trans R Soc Trop Med Hyg* 60:633–649. [http://dx.doi.org/10.1016/0035-9203\(66\)90010-1](http://dx.doi.org/10.1016/0035-9203(66)90010-1).
37. Douradinha B, van Dijk MR, Ataíde R, van Gemert GJ, Thompson J, Franetich JF, Mazier D, Luty AJ, Sauerwein R, Janse CJ, Waters AP, Mota MM. 2007. Genetically attenuated P36p-deficient *Plasmodium berghei* sporozoites confer long-lasting and partial cross-species protection. *Int J Parasitol* 37:1511–1519. <http://dx.doi.org/10.1016/j.ijpara.2007.05.005>.